Stochastic walker with variable long jumps

Upendra Harbola
Department of Inorganic and Physical Chemistry, Indian Institute of Science, Bangalore 560012, India

(Received 29 March 2023; accepted 30 June 2023; published 28 July 2023)

Motivated by recent interest in the stochastic resetting of a random walker, we propose a generalized model where the random walker takes stochastic jumps of lengths proportional to its present position with certain probability, otherwise it makes forward and backward jumps of fixed (unit) length with given rates. The model exhibits a rich stochastic dynamic behavior. We obtain exact analytic results for the first two moments of the walker's displacement and show that a phase transition from a diffusive to superdiffusive regime occurs if the stochastic jumps of lengths that are twice (or more) of its present positions are allowed. This phase transition is accompanied by a reentrant diffusive behavior.

DOI: 10.1103/PhysRevE.108.014135

I. INTRODUCTION

Stochastic dynamics is the fundamental characteristic of a many-body system which has applications in diverse research areas [1,2]. The simplest stochastic walk involves particle dynamics on a one-dimensional (1D) space leading to diffusive dynamics at long times where the mean-squared displacement of the walker grows linearly in time. Several generalizations have been proposed [3–7] to account for the spatial and temporal effects which may lead to nondiffusive dynamics that has been observed in many natural and man-made systems.

A stochastic resetting model has been proposed recently [8] wherein a random walker resets its position at random times to the initial position. This resetting of the position leads to nontrivial qualitative changes in the dynamics of the walker [9–11] which has wide range applications such as in target-search problems [12] and enzymatic activity [13], and has been realized in a recent experiment [14] on the colloidal particles' diffusion using holographic optical tweezers, and a Brown particle dynamics reset using optical tweezers [15]. However, many natural processes, such as the facilitated diffusion of a protein on DNA in the search of a target sequence [16], may involve random hopping of variable lengths to different sites. To account for such processes, we revisit the resetting model in a more general setup and show a rich variety of possibilities that emerge. We start from a microscopic picture using discrete stochastic dynamics and report exact results for the mean and the variance in the general case, which allows us to construct the exact phase diagram for the dynamics of the walker.

II. MODEL AND RESULTS

Consider a random walker in one dimension. At any instant in time t, with the current position at X_t (assuming that the walker starts at time $t = 0$ at $X_0 = 0$), the walker can make jumps of unit length to the left (-1) and to the right $(+1)$ with probability q and p, respectively, and can also jump a length of $-fX_t$, where f is a (positive or negative) factor, with probability r. Thus at any instant in time, $p + q + r = 1$. For the discrete case f is always an integer, but can be a fraction in the continuum limit which we shall discuss later. For $f = 1$, the walker always goes back to the origin and leads to a "stochastic resetting" walk [8]. We note that similar modified resetting walks have been considered in recent works [17,18], where the walker resets its position randomly to a new position such that $0 < f \leqslant 1$. A generalization of the resetting walk $f = 1$ based on the distribution of resetting times has also been considered in a recent work [19]. Here, we present the exact results for transient and asymptotic dynamics of the walker over the full range of f values.

Let $\sigma_t = +1, -1, -fX_{t-1}$ denote the jump at time t which takes the walker to a new position X_t. Then the average length of the first jump, $\langle\sigma_1\rangle = p - q \equiv \alpha$, and the average jump at time t is $\langle\sigma_t\rangle = p - q - rf\langle X_{t-1}\rangle$. Since $X_t = \sum_{k=1}^{t}\sigma_k$, this immediately leads to

$$\langle X_t\rangle = \langle\sigma_t\rangle + \langle X_{t-1}\rangle = \alpha + (1 - rf)\langle X_{t-1}\rangle,$$
$$\langle X_t\rangle = \frac{\alpha}{rf}[1 - (1 - rf)^t]. \tag{1}$$

This is an exact result for the mean position of the walker at time t. Note that if $rf < 2$, the mean position saturates to $\alpha/(rf)$ as $t \to \infty$. However, for $rf > 2$, the walker's mean position $\langle X_t\rangle \sim (-1)^t \frac{\alpha}{rf}(rf)^t$, which changes between positive and negative values with amplitude increasing exponentially with time.

Similarly, using $\langle\sigma_t^2\rangle = (1 - r) + rf^2\langle X_{t-1}^2\rangle$, we obtain

$$\langle X_t^2\rangle = A(r, f, \alpha)(1 + rf^2 - 2rf)^{t-1} + \frac{2\alpha^2}{r^2f^2(f-1)}(1 - rf)^t - \frac{1}{rf(f-2)}\left(\frac{2\alpha^2}{rf} + 1 - r\right), \tag{2}$$

where

$$A(r, f, \alpha) = \left[1 - r - \frac{2\alpha^2}{r^2f^2}\left(\frac{1 - rf}{f - 1} - \frac{1}{f - 2} + \frac{1 - r}{rf(f - 2)}\right)\right].$$

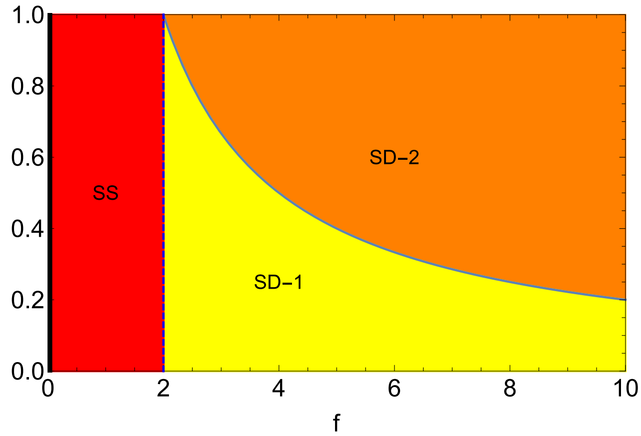

FIG. 1. Phase diagram for the walker. The region filled with red color represents the parameter space where the walker reaches a steady state (SS) at long times. The vertical black line at $f = 0$ and dotted blue line at $f = 2$ denote parameters where the dynamics is diffusive. The blue curve is the locus of points with $rf = 2$ separating the yellow and brown regions denoting two different (SD-1, SD-2) superdiffusive dynamics of the walker.

In the limit $f \to 0$, that is, instead of making jumps with probability r, the walker decides to stay put, $\langle X_t \rangle \to \alpha t$ and $\langle X_t^2 \rangle \to \alpha^2 t^2 + (1 - \alpha^2 - r)t$, leading to a diffusive dynamics with a diffusion coefficient $D = (1 - \alpha^2 - r)/2$.

If $0 < f < 2$, the walker reaches a steady state at asymptotically large times with $\langle X_t \rangle \to \alpha/(rf)$ and $\langle X_t^2 \rangle \to [2\alpha^2 + rf(1 - r)]/[r^2 f^2 (2 - f)]$. For $f = 2$, the walker reenters into a diffusive limit where the mean position reaches a constant $\alpha/(2r)$ while the variance increases linearly in time with diffusion coefficient $D = (1 + \alpha^2/r - r)/2$.

For $f > 2$, there are two scenarios: (i) If $2 < f < 2/r$, the position of the walker at long times saturates to $\alpha/(rf)$ and the variance diverges exponentially, $\langle X_t^2 \rangle \sim A(r, f, \alpha)(1 + rf^2 - 2rf)^{t-1}$, and (ii) when $f > 2/r$, the mean position of the walker oscillates in time around $\alpha/(rf)$ with an exponentially growing amplitude, as is evident from Eq. (1). The second moment, $\langle X_t^2 \rangle$, grows exponentially as in case (i).

The various phases of the walker in its parameter space are shown in Fig. 1. The two distinct diffusive regimes are marked by vertical lines at $f = 0$ and $f = 2$. For $f = 0$, both the mean and the variance grow linearly in time, while for $f = 2$, the mean saturates while the variance show a linear growth in time. In the red region ($0 < f < 2$) the walker reaches a steady state (SS) at long times. In this case, the particle makes jumps that always bring it towards its initial position which mimics the presence of an effective confining potential and thus leads to a steady state. For $f = 2$, these jumps do not lead to any changes in the walker's distance from the initial position and lead to a diffusive dynamics at long times. Two regions of superdiffusion (SD), SD-1 and SD-2, are separated by a curve $r = 2/f$, which is the locus of points where the mean position of the walker fluctuates in time about $\alpha/2$ while the variance diverges exponentially. In region SD-1, the mean position approaches a steady state but the variance increases exponentially in time. In region SD-2, both mean and variance grow exponentially in time.

The probability $P(x, t)$ that the walker is at position $X_t = x$ after (steps) time t satisfies the following rate equation (see the Appendix),

$$P(x, t) = pP(x - 1, t - 1) + qP(x + 1, t - 1) + rP(x/(1 - f), t - 1), \tag{3}$$

with the boundary condition $P(x \to \infty, t) \to 0$. Note that in the random-walk process where $r = 0$, that is, the walker is allowed to make only jumps of unit length each time, $P(x, t) = 0$ for $|x| > t$, and the rate equation can be solved iteratively to get $P(x, t) = (1/2)\,{}^tC_{(t-x)/2}\, p^{(x+t)/2} q^{(t-x)/2}$, which reduces to a Gaussian in the large $t \gg x$ limit. The condition $P(x, t) = 0$ for $|x| > t$ remains valid even for $r \neq 0$ if and only if $f \leqslant 2$. Since in this case the jumps of random lengths do not take the particle further away from the origin, and in order to reach a position at a distance $|x|$, the walker must traverse at least once all the positions lying at the intermediate distances, leading to either a diffusive dynamics or a steady state at long times. For $f > 2$, however, the particle can make jumps of arbitrary lengths that can take the walker further away from the initial point without visiting all intermediate positions, leading to "ultrasuperdiffusive" dynamics where the variance and mean grow exponentially in time. Note that the above conclusions remain valid even if the walker performs ballistic motion ($q = 0$) in between the random variable jumps.

For $f < 0$, the walker always makes random jumps of variable lengths that take it away from the origin. This leads to a monotonically increasing mean position $\langle X_t \rangle$ and $\langle X_t^2 \rangle$ such that the asymptotic dynamics is always superdiffusive.

In Eq. (3), the last term on the right-hand side (rhs) is the contribution to $P(x, t)$ from the jumps of variable lengths. For $f \to 1$, $P(x/(1 - f), t) \to \delta(x)$, reducing to the rate equation for a random walker with "stochastic resetting" [8].

For $t, x \gg 1$, using the Taylor expansion of $P(x \pm 1, t - 1)$ around $P(x, t)$, Eq. (3) can be reduced to a Fokker-Plank (FP) equation for the probability density. For $f = 0$, we obtain

$$\frac{\partial}{\partial t} P(x, t) = -\alpha \frac{\partial}{\partial x} P(x, t) + \frac{1}{2}(1 - r)\frac{\partial^2}{\partial x^2} P(x, t), \tag{4}$$

which has the well-known Gaussian solution

$$P(x, t) = \frac{e^{-\frac{(x-\alpha t)^2}{2t(1-r)}}}{\sqrt{2\pi t(1 - r)}}. \tag{5}$$

Similarly, for the "resetting" walk ($f = 1$) the FP equation is

$$\frac{\partial}{\partial t} P(x, t) = -\frac{\alpha}{1 - r}\frac{\partial}{\partial x} P(x, t) + \frac{1}{2}\frac{\partial^2}{\partial x^2} P(x, t) - \frac{r}{1 - r} P(x, t) + \frac{r}{1 - r}\delta(x), \tag{6}$$

where the first term on the rhs determines the drift of the probability distribution, and the second term is the usual diffusion term. The third and fourth terms are proportional to the parameter r and represent (loss) outflow and (gain) inflow to the probability $P(x, t)$ due to the long jumps.

The solution of the FP Eq. (6) at the steady state leads to the distribution,

$$P(x \geqslant 0) = \frac{r}{1-r} \frac{e^{-x\left(\sqrt{\frac{\alpha^2}{(1-r)^2}+\frac{2r}{1-r}}-\frac{\alpha}{1-r}\right)}}{\sqrt{\frac{\alpha^2}{(1-r)^2}+\frac{2r}{1-r}}}, \tag{7}$$

$$P(x < 0) = \frac{r}{1-r} \frac{e^{x\left(\sqrt{\frac{\alpha^2}{(1-r)^2}+\frac{2r}{1-r}}+\frac{\alpha}{1-r}\right)}}{\sqrt{\frac{\alpha^2}{(1-r)^2}+\frac{2r}{1-r}}}. \tag{8}$$

The steady state is therefore represented by a distribution which falls off exponentially with different rates for $x \geqslant 0$ and $x < 0$, and the difference in the rates is controlled by the parameter α which determines drift in the FP equation. For $\alpha = 0$, the distribution reduces to a simpler form, $P(x) = \sqrt{r/(2-2r)}e^{-|x|\sqrt{2r/(1-r)}}$. As expected, when $r \to 1$, $P(x) \to \delta(x)$ which also follows readily from Eq. (6) as the last two terms on the rhs become dominant as $r \to 1$. Note that the FP Eq. (6) has a different form as compared to the one reported in the literature [8,11]. However, this difference is arising due to the use of a discrete model. If one identifies a diffusion coefficient $D = 1 - r$ and rescales the time t with $t/(1-r)$, Eq. (6) is identical to the one reported in the literature. Nonetheless, Eq. (6) makes the r dependence of the diffusion coefficient explicit, which is not obvious from the equation reported earlier.

Following similar steps, a FP equation can be obtained for $f = 2$ (see the Appendix) which leads to the following approximate distribution function at long times,

$$P(x,t) = \sqrt{\frac{r}{2\pi\gamma t}}\left(1 + \frac{\alpha x}{2\gamma t}\right)e^{-rx^2/(2\gamma t)}, \tag{9}$$

with $\gamma = \alpha^2 + r(1-r)$. This distribution is significantly different from the distribution for $f = 1$, Eqs. (7) and (8). The distribution (9) is peaked at $x = \alpha/(2r)$ which is also the mean value of the walker's position. Thus the mean position saturates while the variance increases linearly in time with rate γ/r. An exact solution for $f = 2$ in the conjugate Fourier space is given by Eqs. (A9) and (A10) in the Appendix.

Note that for $\alpha = 0$, Eq. (9) reduces to a simple Gaussian distribution with zero mean which is identical to the distribution for $f = 0$. Thus, for $\alpha = 0$, the dynamics for $f = 0$ and $f = 2$ are identical. This is because for $f = 2$, the walker makes random transitions from $x \to -x$ with probability r which, for $\alpha = 0$, is the same as staying ($f = 0$) at the current position since $P(x > 0, t) = P(x < 0, t)$. Thus depending on the value of f, the dynamics shows qualitative changes and leads to very different spatial profiles for the distribution function: Gaussian for $f = 0$, exponential for $f = 1$, modified Gaussian for $f = 2$, and power law (see Fig. 2) for $f = 3$.

A numerical solution of Eq. (3) is shown in Fig. 2 for $f = 1, 2$ (diffusion) and $f = 3$ (SD-1) for $p = q = 0.3$ at $t = 30$. Compared to the diffusive region, the distribution function $P(x)$ falls off extremely slowly in the region SD-1. For $f = 3$, we find that the distribution is quite oscillatory and decays according to the power law $\sim(b_0 + x)^{-d_0}$ (shown by the red curve in Fig. 2).

In the standard 1D random walk, the walker visits all positions $<x$ to arrive at the position x. This holds true even for the stochastic walks considered here with $f = 0$ and $f = 1$. However, for $f > 1$, this does not hold true as the long jumps take the walker to a position x from $-x$ without visiting positions between the initial position and the position x. This has interesting consequences on the first-passage-time (FPT) probability $F(x,t)$ [20], the probability density to reach the point x for the first time at time t.

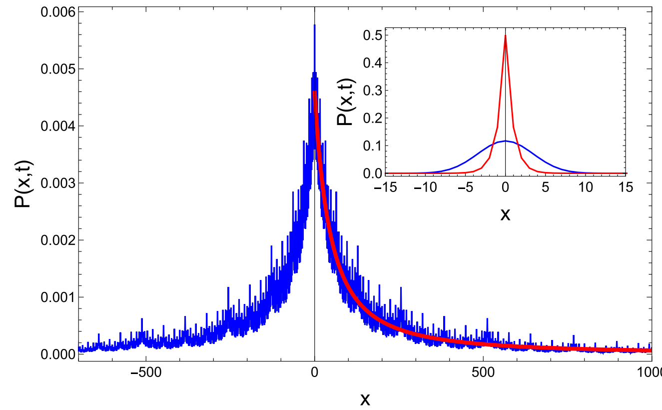

FIG. 2. Probability distribution (blue) at $t = 20$ for $p = q = 0.3$, $r = 0.4$, $f = 3$ obtained from a recursive solution of Eq. (3). The red curve is the fit $a_0(b_0 + x)^{-d_0}$ with $a_0 = 4.212$, $b_0 = 73.677$, $d_0 = 1.587$. The inset shows results for $f = 1.0$ (red) and $f = 2.0$ (blue).

For $f = 0$, from Eq. (4), $F(x,t) = \frac{x}{\sqrt{2\pi(1-r)t^3}}e^{-\frac{(x-\alpha t)^2}{2(1-r)t}}$ which has a form similar to the one obtained for the standard ($r = \alpha = 0$) random walk. However, the crucial difference is in the behavior at a large time. $F(x,t)$ falls off exponentially $F(x,t) \sim e^{-\alpha^2 t/[2(1-r)]}$ at large t and, unlike FPT for the standard random walk, has all its moments well defined. This is to be expected as the mean position of the walker, $\langle x\rangle = \alpha t$, increases linearly with time leading to a faster decay in the probability to visit a position less than the average value for times $t \sim \langle x\rangle/\alpha$. The mean FPT, $\langle t\rangle = (1 - r + 2\alpha x)/(2\alpha^2)$, grows linearly $\sim x/\alpha$ for large x and, as expected, diverges as $\alpha \to 0$.

For $f = 2$,

$$F(x,t) = \frac{r\alpha x^2 + \gamma t(2rx - \alpha)}{4\gamma t^2\sqrt{2\pi\gamma r t}}e^{-\frac{rx^2}{2\gamma t}}, \tag{10}$$

which has a power-law tail $F(x,t) \sim t^{-3/2}$ for large t, similar to the standard case, and therefore has no finite moments. Although the distribution in Eq. (9) is valid for large times and the corresponding FPT distribution, Eq. (10), is valid for $x \geqslant \alpha/(2r)$, both results are exact for $\alpha = 0$.

III. CONCLUSION

In conclusion, a discrete 1D random-walk model is used to obtain exact analytic results for the transient and the asymptotic dynamics of a stochastic walker with random long jumps. The jump lengths are proportional to the position of the walker at the time of the jump. It is found that the asymptotic dynamics depends sensitively on the lengths of jumps and exhibits a rich phase diagram which involves a reentrance of the diffusive dynamics, although of different natures. The exact results obtained here may increase the scope of applications of the resetting walk introduced earlier in the literature.

ACKNOWLEDGMENTS

I thank Prof. B. J. Cherayil for useful discussions and for providing relevant literature in the initial stages of this project. Financial support from SERB, India under Grant No. CRG/2020/0011100 is acknowledged.

APPENDIX: DERIVATION OF THE RATE EQUATION (3)

In order to derive the rate equation (3), we define the characteristic function

$$Q(\lambda, t) = \langle e^{i\lambda X_t}\rangle = \sum_{X_t} e^{i\lambda X_t} P(x, t), \tag{A1}$$

where $P(x, t)$ is the probability to be at $X_t = x$ at time t as defined in the main text. Using $X_t = X_{t-1} + \sigma_t$ and averaging over σ_t, which, due to Markovian dynamics, is independent of X_{t-1}, we get

$$\langle e^{i\lambda X_t}\rangle_{\sigma_t} = e^{i\lambda X_{t-1}} \sum_{n=0}^{\infty} \frac{(i\lambda)^n}{n!} \langle \sigma_t^n \rangle_{\sigma_t}, \tag{A2}$$

where $\langle \cdots \rangle_{\sigma_t}$ is used to denote that the averaging is only over the last step σ_t. Since $\langle \sigma_t^n \rangle_{\sigma_t} = p + (-1)^n + (-1)^n f^n X_{t-1}^n$, we get

$$\begin{aligned}\langle e^{i\lambda X_t}\rangle_{\sigma_t} &= e^{i\lambda X_{t-1}} \sum_{n=0}^{\infty} \frac{(i\lambda)^n}{n!} \langle \sigma_t^n \rangle_{\sigma_t} \\ &= e^{i\lambda X_{t-1}} \left(pe^{i\lambda} + qe^{-i\lambda} + re^{-i\lambda f X_{t-1}}\right). \end{aligned} \tag{A3}$$

Finally, averaging over all X_{t-1} and using Eq. (A1), we get

$$\begin{aligned} Q(\lambda, t) &= pe^{i\lambda} Q(\lambda, t-1) + qe^{-i\lambda} Q(\lambda, t-1) \\ &\quad + rQ(\lambda(1-f), t-1). \end{aligned} \tag{A4}$$

Inverse transforming, $P(x, t) = \int \frac{d\lambda}{2\pi} e^{-i\lambda X_t} Q(\lambda, t)$, and using

$$\begin{aligned} &\int \frac{d\lambda}{2\pi} e^{-i\lambda X_t} Q(\lambda(1-f), t-1) \\ &= \int \frac{d\lambda}{2\pi} e^{-i\lambda X_t} \sum_{X_{t-1}} e^{i\lambda(1-f)X_{t-1}} P(X_{t-1}) \\ &= \sum_{X_{t-1}} P(X_{t-1}) \delta_{X_t, (1-f)X_{t-1}} = P(X_t/(1-f)) \\ &\equiv P(x/(1-f), t-1), \end{aligned} \tag{A5}$$

leads to Eq. (3).

Fokker-Planck equation for $f = 2$

For $f = 2$, the rate equation (3) is $P(x, t) = pP(x-1, t-1) + qP(x+1, t-1) + rP(-x, t-1)$. Using a Taylor expansion around $P(\pm x, t)$, we obtain the following equation for $x \geqslant 0$,

$$\begin{aligned} &\frac{\partial}{\partial t} P(x, t) + \frac{r}{1-r} \frac{\partial}{\partial t} P(-x, t) \\ &= -\frac{\alpha}{1-r} \frac{\partial}{\partial x} P(x, t) + \frac{1}{2} \frac{\partial^2}{\partial x^2} P(x, t) \\ &\quad - \frac{r}{1-r} [P(x, t) - P(-x, t)]. \end{aligned} \tag{A6}$$

A conjugate equation for $x < 0$ can be obtained by replacing $x \to -x$ in the above equation. Note that $P(x, t)$ and $P(-x, t)$ are not conserved as the walker can make random jumps from left to right and vice versa. The sum of the probability $P_+(x, t) = P(x, t) + P(-x, t)$ is however conserved and follows a coupled FP equation,

$$\frac{\partial P_+(x, t)}{\partial t} = \frac{1}{2}(1-r) \frac{\partial^2 P_+(x, t)}{\partial x^2} - \alpha \frac{\partial}{\partial x} P_-(x, t). \tag{A7}$$

The difference $P_-(x, t) = P(x, t) - P(-x, t)$ satisfies the following coupled equation,

$$\begin{aligned} \frac{\partial}{\partial t} P_-(x, t) &= \frac{1}{2} \frac{1-r}{1-2r} \frac{\partial^2}{\partial x^2} P_-(x, t) - \frac{2r}{1-2r} P_-(x, t) \\ &\quad - \frac{\alpha}{1-2r} \frac{\partial}{\partial x} P_+(x, t). \end{aligned} \tag{A8}$$

Equations (A7) and (A8) are solved in a Fourier domain to obtain

$$\begin{aligned} P_+(k, t) &= 2e^{-t\frac{2r+k^2(1-r)^2}{2(1-2r)}} \left[\cosh\left(\frac{t\lambda}{2(1-2r)}\right) \right. \\ &\quad \left. + \frac{2r + k^2 r(1-r)}{\lambda} \sinh\left(\frac{t\lambda}{2(1-2r)}\right)\right], \end{aligned} \tag{A9}$$

where we have used $P_+(k, 0) = 2$ and

$$\lambda = \sqrt{r^2[k^2(1-r)+2]^2 - 4k^2\alpha^2(1-2r)}.$$

Similarly,

$$P_-(k, t) = \frac{4i\alpha k}{\lambda} e^{-t\frac{2r+k^2(1-r)^2}{2(1-2r)}} \sinh\left(\frac{t\lambda}{2(1-2r)}\right). \tag{A10}$$

Note that for $\alpha = 0$, $P_-(k, t) = 0$, that is, $P(x, t) = P(-x, t)$, as expected. $P_+(x, t)$ is then identical to the distribution for the $f = 0$ case. This is because for $f = 2$, the walker makes random long jumps from $x \to -x$ (and vice versa) with probability r, which is the same as remaining at x with probability r since the dynamics in the $x \geqslant 0$ space are identical to the one in $x < 0$ space for $\alpha = 0$.

Next, in order to compute the distribution in real space, $P(x, t)$, we compute the Fourier transform of $P_+(k, t)$ and $P_-(k, t)$. We perform this transformation approximately by expanding the hyperbolic cosine and sine functions near $k = 0$,

$$\begin{aligned} \cosh\left(\frac{t\lambda}{2(1-2r)}\right) &\approx \cosh\left(\frac{rt}{1-2r}\right) e^{\frac{r(1-r)}{2(1-2r)}\gamma_1 t k^2}, \\ \frac{1}{\lambda}\sinh\left(\frac{t\lambda}{2(1-2r)}\right) &\approx \frac{1}{2r}\sinh\left(\frac{rt}{1-2r}\right) e^{\frac{r(1-r)}{2(1-2r)}\gamma_2 t k^2} \\ &\quad \times e^{-\frac{1}{2}(1-r)\gamma k^2}, \end{aligned} \tag{A11}$$

where $\gamma = 1 - \alpha^2(1-2r)/[r^2(1-r)]$, $\gamma_1 = \gamma \tanh[tr/(1-2r)]$, and $\gamma_2 = \gamma \coth[tr/(1-2r)]$. A small k expansion in Eq. (A11) is expected to work well at large times since it appears together with a Gaussian function in k which dominates at small k at large times.

This leads to

$$P_+(x,t) = 2\sqrt{\frac{1-2r}{2\pi t(1-r)\beta_2}}e^{-\frac{rt}{1-2r}}\sinh\left(\frac{rt}{1-2r}\right)\left[\sqrt{\frac{\beta_2}{\beta_1}}\coth\left(\frac{rt}{1-2r}\right)e^{-\frac{1-2r}{2t\beta_1(1-r)}x^2} + \left(1+\frac{1-2r}{2t\beta_2} - \frac{(1-2r)^2x^2}{2(1-r)\beta_2^2t^2}\right)e^{-\frac{1-2r}{2t\beta_2(1-r)}x^2}\right], \tag{A12}$$

$$P_-(x,t) = \frac{2\alpha}{\sqrt{2\pi}\,r}\left(\frac{1-2r}{(1-r)t\beta_2}\right)^{\frac{3}{2}}e^{-\frac{tr}{1-2r}}\sinh\left(\frac{rt}{1-2r}\right)xe^{-\frac{1-2r}{2t\beta_2(1-r)}x^2}, \tag{A13}$$

where $\beta_1 = 1 - r(1+\gamma_1)$ and $\beta_2 = 1 - r(1+\gamma_2) + \gamma(1-2r)/t$. Note that for $t \to 0$, $t\beta_1$ approaches zero as $\to t(1-r)$ while $t\beta_2 \to \gamma(1-2r)$. This results in $P_-(x, t \to 0) = 0$ and $P_+(x, t \to 0) = 2\delta(x)$. In the limit when t is large such that $e^{-tx}\sinh(tx) \to 1/2$ and $\coth(tx) \to 1$, $\beta_1 = \beta_2 \to (1-2r)[\alpha^2 + r(1-r)]/(r-r^2)$. In this long-time limit, Eqs. (A12) and (A13) reduce to

$$P_+(x,t) = 2\left(1 + \frac{r(1-r)}{4t[\alpha^2+r(1-r)]} - \frac{r^2(1-r)}{4[\alpha^2+r(1-r)]^2}\frac{x^2}{t^2}\right)\sqrt{\frac{r}{2\pi t[\alpha^2+r(1-r)]}}e^{-\frac{r}{2t[\alpha^2+r(1-r)]}x^2}, \tag{A14}$$

$$P_-(x,t) = \frac{\alpha}{r\sqrt{2\pi}}\left(\frac{r}{t[\alpha^2+r(1-r)]}\right)^{\frac{3}{2}}xe^{-\frac{r}{2t[\alpha^2+r(1-r)]}}. \tag{A15}$$

Further, for large t, if we ignore the last two terms inside the parentheses in $P_+(x,t)$ in Eq. (A14) and use $P(x,t) = [P_+(x,t) + P_-(x,t)]/2$, we get the result reported in Eq. (9) in the main text.

[1] S. Chandrasekhar, Rev. Mod. Phys. **15**, 1 (1943).
[2] G. Drazer and D. H. Zanette, Phys. Rev. E **60**, 5858 (1999); R. N. Ghosh and W. W. Webb, Biophys. J. **66**, 1301 (1994); J. G. Skellam, Biometrika **38**, 196 (1951); M. G. Bruno, P. Allegrini, and P. Grigolini, Appl. Stoch. Models Bus. Ind. **15**, 235 (1999).
[3] P. Hönggi, Z. Phys. B **31**, 407 (1978).
[4] V. S. Volkov and V. N. Pokrovsky, J. Math. Phys. **24**, 267 (1983).
[5] R. Metzler, E. Barkai, and J. Klafter, Phys. Rev. Lett. **82**, 3563 (1999).
[6] N. Madras and G. Slade, *The Self Avoiding Walk* (Birkhauser, Boston, 1993).
[7] U. Harbola, N. Kumar, and K. Lindenberg, Phys. Rev. E **90**, 022136 (2014).
[8] M. R. Evans and S. N. Majumdar, Phys. Rev. Lett. **106**, 160601 (2011).
[9] S. N. Majumdar, S. Sabhapandit, and G. Schehr, Phys. Rev. E **91**, 052131 (2015).
[10] M. R. Evans, S. N. Majumdar, and G. Schehr, J. Phys. A: Math. Theor. **53**, 193001 (2020).
[11] S. Gupta and A. M. Jayannavar, Front. Phys. **10**, 789097 (2022).
[12] A. J. Bray, S. N. Majumdar, and G. Schehr, Adv. Phys. **62**, 225 (2013).
[13] S. Reuveni, M. Urbakh, and J. Klafter, Proc. Natl. Acad. Sci. USA **111**, 4391 (2014).
[14] O. Tal-Friedman, A. Pal, A. Sekhon, S. Reuveni, and Y. Roichman, J. Phys. Chem. Lett. **11**, 7350 (2020).
[15] B. Besga, A. Bovon, A. Petrosyan, S. N. Majumdar, and S. Ciliberto, Phys. Rev. Res. **2**, 032029 (2020).
[16] S. E. Halford and J. F. Marko, Nucleic Acids Res. **32**, 3040 (2004).
[17] O. Tal-Friedman, Y. Roichman, and S. Reuveni, Phys. Rev. E **106**, 054116 (2022).
[18] J. K. Pierce, arXiv:2204.07215.
[19] R. K. Singh, K. Górska, and T. Sandev, Phys. Rev. E **105**, 064133 (2022).
[20] G. H. Weiss, Adv. Chem. Phys. **13**, 1 (1967).